RSC Advances

PAPER

View Article Online
View Journal | View Issue

Cite this: *RSC Adv.*, 2017, **7**, 25821

An octanuclear Schiff-base complex with a Na_2Ni_6 core: structure, magnetism and DFT calculations†

Marek Machata, Ivan Nemec, Radovan Herchel and Zdeněk Trávníček *

Received 2nd February 2017
Accepted 2nd May 2017

DOI: 10.1039/c7ra01374d

rsc.li/rsc-advances

The octanuclear Na_2Ni_6 complex $(Pr_3NH)[Na_2Ni_6(L)_4(Bza)_5(HBza)(OH)_2(ace)]\cdot Et_2O$ (**1**), where Pr_3NH^+ = the tripropylamonium cation, H_2L = 2-[(*E*)-(2-hydroxybenzylidene)amino]phenol, HBza = benzoic acid and ace = acetone, was synthesized and characterized by the elemental analysis, FTIR spectroscopy, single crystal X-ray diffraction analysis, magnetic measurements and DFT calculations. All six Ni^{II} atoms are hexacoordinate with the $\{NiO_6\}$ or $\{NiNO_5\}$ chromophores forming two defective dicubane cores. The static magnetic data were fitted to the simplified spin Hamiltonian model which resulted in averaged ferromagnetic and antiferromagnetic exchange parameters J = +5.3 cm^{-1}, and J = −9.2 cm^{-1}, respectively, confirming the predominant role of the antiferromagnetic coupling in **1**. The broken symmetry DFT method with various functionals (B3LYP, PBE0, TPPSh and CAM-B3LYP) was used to dissect information about magnetic coupling. As a result, the isotropic exchange parameters (J_{ab}) derived by the PBE0 or B3LYP functionals seem to be the best to match the experimental magnetic data.

Introduction

Since the discovery of the first single-molecule magnets (SMMs),[1] paramagnetic transition and inner transition metal complexes have been the subject of research interest in the field of molecular magnetism.[2] In order to obtain SMMs, a non-zero spin ground state and non-negligible easy-axis magnetic anisotropy are required. Thus, two basic strategies, that can lead to the preparation of such compounds, can be recognized. The first approach is aimed at modulation of the magnetic anisotropy to favourable value and type (large, and axial, respectively) by careful choice of the ligands and symmetry of mononuclear complexes.[3,4] In the recent works a very large single ion magnetic anisotropy of the Ni^{II} atoms was observed, nevertheless, the slow relaxation of magnetization in mononuclear Ni^{II} complexes is still observed only very rarely.[5] The second strategy is aimed at preparation of the polynuclear complexes with well-separated and large ground spin state.[6] Potential drawbacks of the latter strategy arise from predominant antiferromagnetic coupling[7] and/or decrease of magnetic anisotropy due to different orientations of the local atomic D-tensors.[2d,8,9] Thus, up to now, only a few homometalic and polynuclear Ni^{II} SMMs have been reported.[7,10,11] Nevertheless, the research in the field of high-nuclear Ni^{II} complexes has brought the compounds with various structures such as wheels,[12] grids,[13] cages[11b,14] or cubanes.[7,11c–g,15] Interestingly, the majority of the Ni^{II} SMMs were reported for the cubanes.[7,11c–g] This might be attributed to the orthogonality of magnetic orbitals in such compounds as the bonding angles between the bridged metal centers are close to 90° favouring thus ferromagnetic coupling.[16]

In our previous work[9] we have reported on the crystal structure and magnetic properties of two new tetranuclear Ni^{II} compounds: $[Ni_4(L)_4(CH_3OH)_3(H_2O)]$ and $(Pr_3NH)_2[Ni_4(L)_4(ac)_2]$, where Pr_3NH^+ = the tripropylamonium cation, H_2L = 2-[(*E*)-(2-hydroxybenzylidene)amino]phenol and Hac = acetic acid. We have shown that the used reaction solvent (*i.e.* CH_3OH and/or CH_2Cl_2 in this case) strongly influence composition and topology of the polynuclear clusters despite using the same reactants and their ratios. Also, the magnetic properties of the above mentioned compounds differ significantly and $(Pr_3NH)_2[Ni_4(L)_4(ac)_2]$ exhibits a field-induced slow relaxation of magnetization. Furthermore, it must be noted that also other previously reported 3d,[17] 3d-4f[18] or 4f[19] polynuclear compounds with the H_2L (and related) ligands exhibit interesting magnetic properties. With respect to the above mentioned facts and as a continuation of our ongoing study of polynuclear Ni^{II} compounds, we report here on the synthesis, crystal structure and magnetic properties of the octanuclear cubane-based complex of the formula $(Pr_3NH)[Na_2Ni_6(L)_4(Bza)_5(HBza)(OH)_2(ace)]\cdot Et_2O$ (**1**), where HBza = benzoic acid, ace = acetone. The evaluation of magnetic properties was supported by thorough theoretical investigations utilizing a broken-symmetry DFT method with the B3LYP, PBE0, TPPSh and CAM-B3LYP functionals.

Department of Inorganic Chemistry, Regional Centre of Advanced Technologies and Materials, Faculty of Science, Palacký University, 17. listopadu 12, CZ-771 46 Olomouc, Czech Republic. E-mail: zdenek.travnicek@upol.cz

† Electronic supplementary information (ESI) available. CCDC 1530435. For ESI and crystallographic data in CIF or other electronic format see DOI: 10.1039/c7ra01374d

Results and discussion

Synthesis and crystal structure

Compound **1** (Fig. 1) was prepared by one-pot synthesis using $NiCl_2 \cdot 6H_2O$, the Schiff base ligand H_2L in the presence of sodium benzoate and Pr_3N as bases (molar ratios: 1.5 : 1:3 : 2), and acetone as the reaction solvent, see the eqn (1). Note: the molar ratios of the reactants mentioned above differ from those given in the eqn (1). This may be associated with the fact that the organic reactants behave as weak acids or bases which influences the chemical equilibria in solution during the reaction.

$$6NiCl_2 + 4H_2L + 8NaBza + 7Pr_3N + 2H_2O + ace \rightleftarrows (Pr_3NH)[Ni_6Na_2(L)_4(Bza)_5(HBza)(OH)_2(ace)] + 6(Pr_3NH)Cl + 6NaCl + 2HBza \quad (1)$$

The complex **1** crystallizes in the monoclinic space group $P2_1/c$ and comprises the Pr_3NH^+ cation, octanuclear complex anion $[Na_2Ni_6(L)_4(Bza)_5(HBza)(OH)_2(ace)]^-$ and co-crystalized Et_2O molecule. Basic crystal data, structure refinement parameters, and selected bond lengths and angles are listed in Tables S1, S2, and Fig. S1 (in ESI†), respectively. The complex anion (Fig. 1) is composed of six Ni^{II} atoms, two Na^+ atoms, four deprotonated L^{2-} ligands, two μ^3-OH^- and five Bza^- anionic ligands, one HBza and acetone (ace) coordinated molecules. All the Ni^{II} atoms are incorporated in two defective dicubane cores mutually connected by one face with the bridging (vertex) phenolate oxygen atoms (O_{Ph}) and the hydroxo ligands (O_{Hy}). The remaining coordination sites are occupied by the oxygen atoms originating from the carboxylate ligands (O_{Ca}), which adopt various bridging modes ($2 \times \eta^2{:}\eta^1{:}\mu^2$, $1 \times \eta^1{:}\eta^1{:}\mu^2$, $2 \times \eta^1{:}\eta^2{:}\mu^3$ and $1 \times \eta^1$, Fig. 1 and 2), and one acetone molecule. All the Ni^{II} atoms are hexacoordinate, but they differ in the composition of their coordination polyhedra: $\{NiO_6\}$ for the Ni4 and Ni6 atoms, $\{NiNO_5\}$ for the remaining ones (Fig. 1).

Furthermore, another difference between the Ni central atoms is observed. The coordination polyhedra of the Ni1 and Ni5 atoms are less angularly distorted (as defined by the parameter Σ,[20] 63.47° and 77.80°) than the remaining ones (96.8–119.4°). The bonding distances (in Å) within the coordination polyhedra of the Ni^{II} atoms vary in the range of 1.98–2.19 for the Ni–O and 1.99–2.03 for Ni–N bonds.

The Na^+ atoms are hexacoordinate, coordinated solely by the oxygen atoms with the bond distances (in Å) ranging from 2.26 to 3.04. The O_{Ph} atoms are not equivalent from the view of their bridging functions and the asymmetry of L^{2-}, which implies the aforementioned non-equivalency, as was discussed previously.[18] In **1**, the O_{Ph} atoms originating from the aldehydic part of the ligand L^{2-} adopt μ bridging mode while the aminophenolic O_{Ph} atoms bridges three Ni^{II} atoms (μ^3, Fig. 1 and 2). These atoms connect defective dicubane cores with Na^+ atoms as well. Bond angles between the double oxo-bridged Ni^{II} atoms (in °) are ranging from 90.7 to 94.9 (Ni1–O–Ni2, Ni1–O–Ni4, Ni2–O–Ni3, Ni3–O–Ni5, Ni5–O–Ni6) and from 99.0 to 105.0 (Ni1–O–Ni3, Ni2–O–Ni5, Ni2–O–Ni6, Ni3–O–Ni4). Furthermore, the Ni atoms are not bridged solely by the double oxo-bridging oxygen atoms. Between the Ni1 and Ni4, and Ni5 and Ni6 atoms the additional $\eta^1{:}\eta^2{:}\mu^3$ bridging by the Bza^- ligands (involving also bond with adjacent sodium atom, Fig. 2) takes place (Fig. 1).

The molecular structure of the complex anion is stabilized by two rather strong intramolecular hydrogen bonds between two μ^3-OH groups and one O_{Ca} atom (from *syn–anti* – benzoate

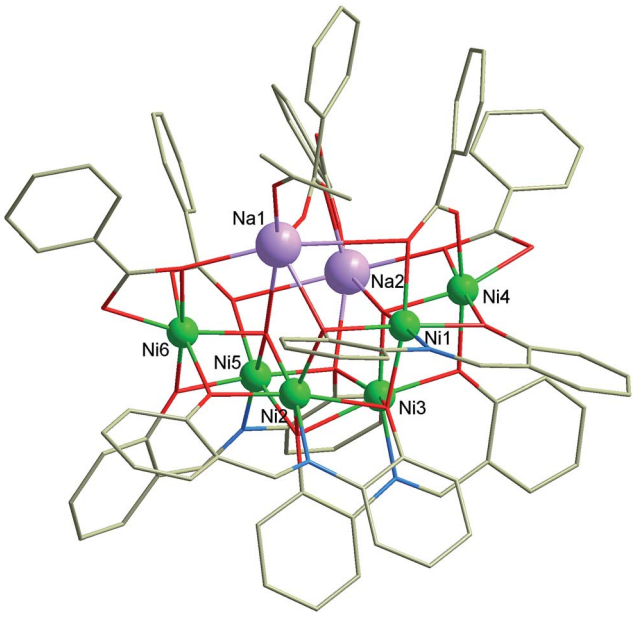

Fig. 1 Molecular structure of the complex anion $[Na_2Ni_6(L)_4(Bza)_5(HBza)(OH)_2(ace)]^-$. Color code: bright green (Ni), violet (Na), red (O), blue (N), grey (C). Hydrogen atoms are omitted for clarity.

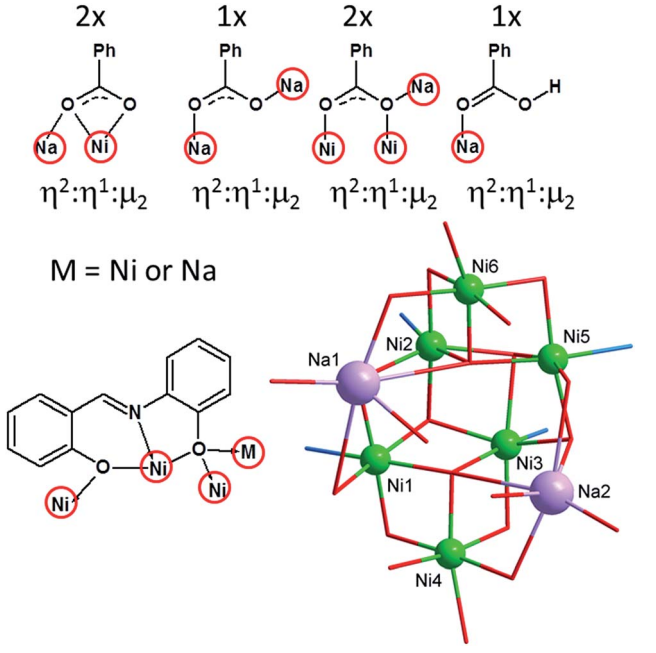

Fig. 2 View of the bridging abilities of the benzoato (up) and H_2L (down left) ligands, and simplified picture showing all the coordination polyhedrons and labelling of the metal atoms in **1** (down right).

ligand bridging two Na atoms) with $d(O\cdots O) = 2.863(6)$ and 2.927(5) Å. The complexity of the molecular structure which was described above is not surprising in context of the bridging abilities of the H_2L-type ligands (Fig. 2). The reactions of the Ni^{II} salts with the H_2L-type ligands led previously to the preparation of cubane and defective dicubane Ni_4 compounds,[9,21] tetra and hexanuclear $NaNi_3$ and $NaNi_5$ compounds,[17b] or even Ni_{20} compound with bowl topology.[22]

There are no significant intermolecular contacts between the adjacent complex anions in the crystal structure and the shortest distance between the Ni^{II} atoms (in Å) of the adjacent complex anions is 9.6342(11). The only significant intermolecular contact is the N–H···O hydrogen bond between the tripropylamonium cation (donor) and the carboxylate group of the complex anion (acceptor) with the distance of 3.007(12) Å (Fig. S2 in ESI†).

Magnetic studies and DFT calculations

Variable-temperature dc magnetic data (Fig. 3, left) measured from 1.9 to 300 K showed room temperature value of μ_{eff}/μ_B equal to 7.55, which is consistent with six uncoupled Ni^{II} atoms with $g = 2.16$. The effective magnetic moment remains constant down to approximately 75 K and on further cooling it drops to 2.53 μ_B at $T = 1.9$ K. Such behaviour suggests presence of predominant antiferromagnetic coupling in **1**.

Variable-field dc data (Fig. 3, right) measured up to 5 T do not display saturation most probably because there are close-lying spin states with various molecular spins affected also by magnetic anisotropy. In order to interpret magnetic data for **1**, we postulated the following spin Hamiltonian

$$\begin{aligned}\hat{H} = &-J_{12}(S_1\cdot S_2) - J_{13}(S_1\cdot S_3) - J_{14}(S_1\cdot S_4) - J_{23}(S_2\cdot S_3)\\ &-J_{25}(S_2\cdot S_5) - J_{26}(S_2\cdot S_6) - J_{34}(S_3\cdot S_4) - J_{35}(S_3\cdot S_5)\\ &-J_{56}(S_5\cdot S_6) + \mu_B\sum_{i=1}^{6} B\cdot g_i\cdot S_i \end{aligned} \quad (2)$$

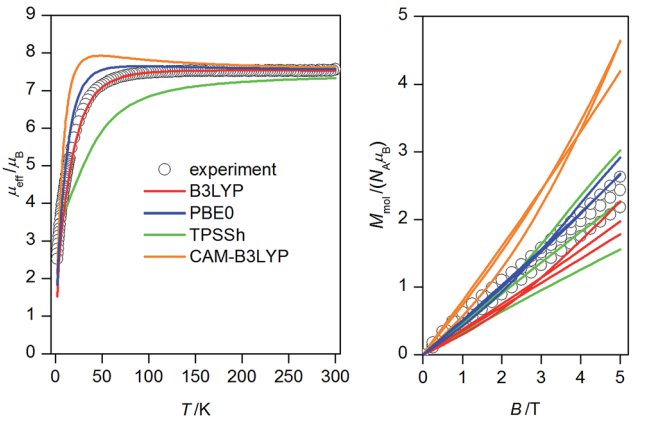

Fig. 3 Magnetic data for **1**: temperature dependence of the effective magnetic moment recorded under 0.1 T (left) and the isothermal magnetizations measured at 2, 5 and 10 K (right). Empty circles – experimental data, full lines – calculated data with J_{ab} parameters resulted from DFT calculations listed in Table 1 and $g = 2.16$.

where the isotropic exchange interactions J_{ab} among the adjacent nickel atoms bridged by the phenolato or hydroxido ligands were considered together with Zeeman term (Fig. 4). However, there are too many free parameters to simply fit the experimental magnetic data and there is no simple magneto-structural correlation available for this system, which could be used to reduce number of J_{ab}.

Therefore, we utilized Density Functional Theory (DFT) with the broken-symmetry approach to at least estimate values and nature of J_{ab} in **1** and eventually facilitate the analysis of the magnetic properties following our previous works on polynuclear compounds.[23] Herein, the ORCA computation package 3.0.3 was employed for all the calculations and polarized triple-zeta basis set def2-TZVP(-f) was used for all the atoms except for carbon and hydrogen atoms, for which def2-SVP basis set was used. The calculations were done for the molecular fragment $(Pr_3NH)[Na_2Ni_6(L)_4(Bza)_5(HBza)(OH)_2(ace)]$ of **1** (Fig. 5). The broken-symmetry spin states (BS) need to be calculated and their energies compared to the energy of the high spin state (HS) in order to compute J-parameters. Herein, the Ruiz's approach was employed to derive the following relationships

$$\begin{aligned} J_{12} &= (\Delta_1 + \Delta_2 - \Delta_{12})/6\\ J_{13} &= (\Delta_1 - \Delta_2 + \Delta_3 - \Delta_4 + \Delta_{12} - \Delta_{34})/6\\ J_{14} &= (-\Delta_3 + \Delta_4 + \Delta_{34})/6\\ J_{23} &= (-\Delta_1 + \Delta_2 + \Delta_{34} - \Delta_{56})/6\\ J_{25} &= (\Delta_5 - \Delta_6 + \Delta_{12} - \Delta_{34})/6\\ J_{26} &= (-\Delta_5 + \Delta_6 + \Delta_{56})/6\\ J_{34} &= (\Delta_3 + \Delta_4 - \Delta_{34})/6\\ J_{35} &= (-\Delta_{12} + \Delta_{34} + \Delta_{56})/6\\ J_{56} &= (\Delta_5 + \Delta_6 - \Delta_{56})/6 \end{aligned} \quad (3)$$

where $\Delta_i = \varepsilon_{BS,i} - \varepsilon_{HS}$. We have tested several DFT functionals, hybrid functionals B3LYP and PBE0, meta-hybrid functional TPSSh and also range-separated hybrid functional CAM-B3LYP.

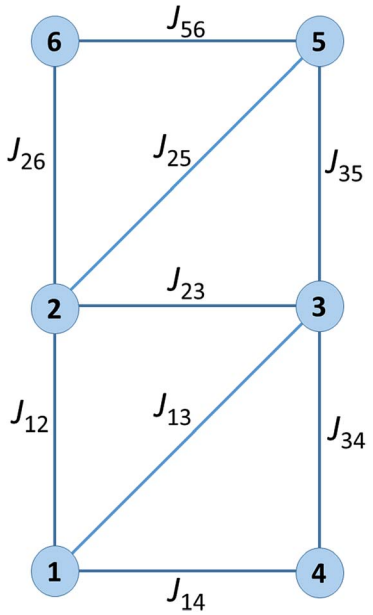

Fig. 4 Scheme of the magnetic coupling in **1**.

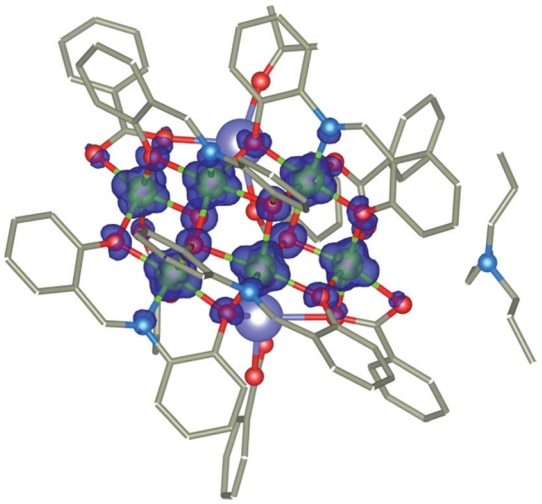

Fig. 5 The molecular fragment $(Pr_3NH)[Na_2Ni_6(L)_4(Bza)_5(HBza)(OH)_2(ace)]$ of **1** and B3LYP calculated spin isodensity surface for high spin state with the cutoff values of 0.01 e a_0^{-3}. Hydrogen atoms are omitted for clarity.

The resulting J_{ab} parameters are listed in Table 1 for all the above mentioned functionals and the details for the B3LYP functional are listed in Table 2. It follows from Table 1 that all the functionals (B3LYP, PBE0, TPPSh and CAM-B3LYP) provided consistent sets of J-parameters concerning their nature, concretely, $J_{12}, J_{14}, J_{23}, J_{35}$ and J_{56} are all ferromagnetic, and the J_{13}, J_{25}, J_{26} and J_{34} are all antiferromagnetic.

Table 1 The comparison of the calculated isotropic exchange parameters J_{ab} (cm^{-1}) for **1** using various DFT functionals

	B3LYP	PBE0	TPSSh	CAM-B3LYP
J_{12}	+10.5	+8.86	+9.63	+9.39
J_{13}	−6.72	−4.69	−13.2	−2.50
J_{14}	+16.9	+15.1	+14.7	+15.6
J_{23}	+13.8	+11.9	+13.3	+12.0
J_{25}	−12.4	−8.87	−20.7	−7.11
J_{26}	−14.2	−9.26	−25.9	−6.49
J_{34}	−14.1	−9.47	−25.0	−7.02
J_{35}	+7.48	+6.77	+4.64	+7.52
J_{56}	+16.0	+13.8	+14.8	+14.2

Table 2 B3LYP/def2-TZVP(-f)/def2-SVP calculated $\langle S^2 \rangle$ values and relative energies of broken-symmetry (BS) spin states for $(Pr_3NH)[Na_2Ni_6(L)_4(Bza)_5(HBza)(OH)_2(ace)]$ of **1**[a]

Spin state	$\langle S^2 \rangle$	Δ_i (cm^{-1})
HS, $\|\alpha\alpha\alpha\alpha\alpha\alpha\rangle$	42.02	0
BS1, $\|\beta\alpha\alpha\alpha\alpha\alpha\rangle$	22.02	62.030
BS2, $\|\alpha\beta\alpha\alpha\alpha\alpha\rangle$	22.01	−6.932
BS3, $\|\alpha\alpha\beta\alpha\alpha\alpha\rangle$	22.01	1.305
BS4, $\|\alpha\alpha\alpha\beta\alpha\alpha\rangle$	22.02	8.281
BS5, $\|\alpha\alpha\alpha\alpha\beta\alpha\rangle$	22.02	33.140
BS6, $\|\alpha\alpha\alpha\alpha\alpha\beta\rangle$	22.02	5.228
BS12, $\|\beta\beta\alpha\alpha\alpha\alpha\rangle$	10.01	−7.901
BS34, $\|\alpha\alpha\beta\beta\alpha\alpha\rangle$	10.02	94.419
BS56, $\|\alpha\alpha\alpha\alpha\beta\beta\rangle$	10.01	−57.427

[a] $\Delta_i = \varepsilon_{BS,i} - \varepsilon_{HS}$.

Next, the obtained four sets of J's values from each DFT functional were afterwards used to calculate magnetic properties of **1** with the spin Hamiltonian in the eqn (2). The calculated magnetic data are depicted in Fig. 3, from which we may conclude that PBE0 and B3LYP derived J-parameters delivered the best agreement with the experiment.

The CAM-B3LYP functional seems to slightly overestimate effect of the ferromagnetic exchanges, whereas TPPSh overestimates the effect of the antiferromagnetic exchanges. Furthermore, the attempt to find the magneto-structural correlations was done for PBE0-derived parameters as outlined in Fig. 6, where a linear equation of the form

$$J\ (\mathrm{cm}^{-1}) = 196(30) - 1.99(31)\cdot\alpha \qquad (4)$$

was found using the average Ni–O–Ni angles (calculated as average value of two Ni–O–Ni angles within the double oxo-bridged pair) as a parameter α with the correlation coefficient $R^2 = 83.3$. The relationship predicts the borderline between the ferromagnetic and the antiferromagnetic exchange parameters to be at $\alpha = 98.5°$. This is in a very good agreement with the magneto-structural correlations found for the Ni_4 cubane compounds previously, in which the relationship between the experimentally-derived J value and Ni–O–Ni angle is also linear with $\alpha \approx 99°$.[9,16,24]

Taking into the account that both PBE0 and B3LYP derived antiferromagnetic and ferromagnetic J-parameters are in more less narrow interval, the experimental magnetic data were analysed also with very simplified model using only two J-parameters, thus averaging the ferromagnetic exchanges ($J_F = J_{12} = J_{14} = J_{23} = J_{35} = J_{56}$) and the antiferromagnetic exchanges ($J_{AF} = J_{13} = J_{25} = J_{26} = J_{34}$). Under this assumption, good agreement with the experimental data was achieved for $J_F = +5.3$

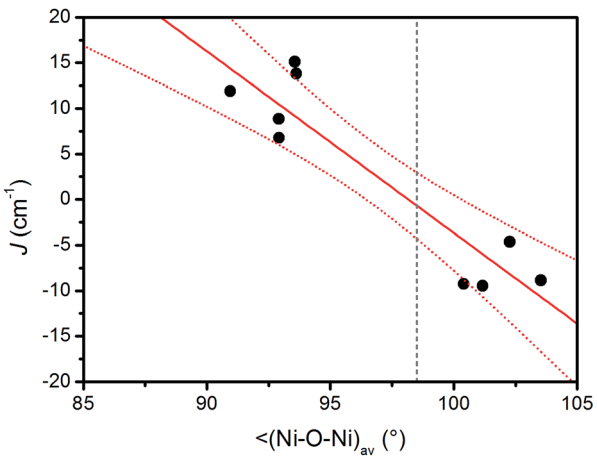

Fig. 6 A magneto-structural correlation, J vs. α, $\alpha = <(Ni–O–Ni)_{av}$, for the PBE0-calculated J-parameters. The confidence interval with 95% is shown (dotted lines). The grey dashed lined represents predicted borderline between the ferromagnetic and the antiferromagnetic exchange parameters.

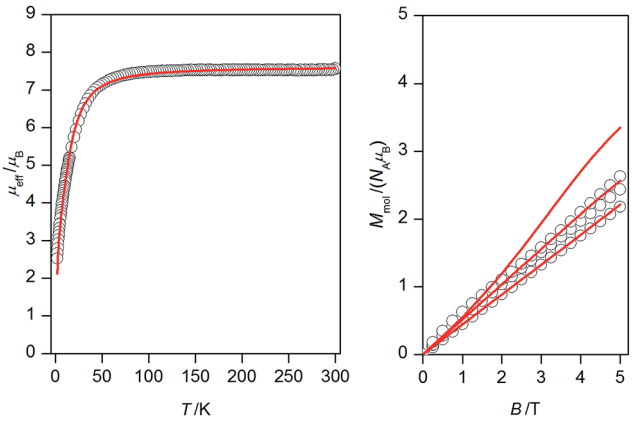

Fig. 7 Magnetic data for **1**: temperature dependence of the effective magnetic moment recorded under 0.1 T (left) and the isothermal magnetizations measured at 2, 5 and 10 K (right). Empty circles – experimental data, full lines – calculated data with $J_F = +5.3$ cm^{-1} and $J_{AF} = -9.2$ cm^{-1} and $g = 2.20$.

cm^{-1} and $J_{AF} = -9.2$ cm^{-1} and $g = 2.20$ (Fig. 7). Both temperature and field dependent magnetic data are well described by this model, only calculated data for the isothermal magnetization at $T = 2$ K are a bit higher than the experimental one, which can be due the simplicity of the model and also due to expected significant single-ion zero-field splitting for Ni^{II} ions in deformed octahedral coordination environment, which usually leads to lower saturation values of the isothermal magnetization.[25]

Conclusions

In conclusion, we have prepared a heterobimetallic complex $(Pr_3NH)[Na_2Ni_6(L)_4(Bza)_5(HBza)(OH)_2(ace)]\cdot Et_2O$, (**1**). Its crystal structure revealed that the paramagnetic Ni^{II} atoms are arranged in two defective dicubane cores. Due to the structural complexity, implying the magnetic exchange interactions in **1**, a few DFT functionals (B3LYP, PBE0, TPSSh, CAM-B3LYP) in combination with the def2-TZVP(-f) and def2-SVP basis sets were utilized for calculations of magnetic coupling parameters. It has been shown that the PBE0 and B3LYP methods provide the best estimates of J_{ab}. The nature of the magnetic exchanges is governed by the average Ni_a-O-Ni_b angle with the estimated crossing point of the ferromagnetic and antiferromagnetic values at $\alpha = 98.5°$, and this value is in good agreement with that obtained using the magneto-structural correlations ($\alpha \approx 99°$) reported for the Ni_4-cubane compounds previously. Utilizing the theoretical calculations, the simplification of the spin Hamiltonian parameters was suggested leading to the fitted average isotropic exchange parameters, $J_F = +5.3$ cm^{-1} and $J_{AF} = -9.2$ cm^{-1} confirming the predominant role of the antiferromagnetic coupling in **1**.

Experimental section

Synthesis

All used chemicals and solvents were purchased from commercial sources and were used without any further purification. The ligand H_2L was prepared as reported previously.[26]

$(Pr_3NH)[Na_2Ni_6(L)_4(Bza)_5(HBza)(OH)_2(ace)]\cdot Et_2O$ (1). Solid sodium benzoate (1.5 mmol, 0.218 g) was added to a green mixture of H_2L (0.5 mmol, 0.107 g) and $NiCl_2$ (0.8 mmol, 0.178 g, used as a hexahydrate) in acetone (20 mL). The resulted mixture was stirred at boiling point for 15 min and then the solution of Pr_3N (1 mmol, 0.143 g) in acetone (5 cm^3) was added dropwise. Then, the mixture was filtered and left at room temperature to evaporate to dryness. After 3 weeks the greenish solid was obtained. It was dissolved in acetone (20 cm^3) and left to crystallize by slow diffusion of Et_2O for 2 days. The dark green crystals were collected by filtration. Yield: 24% (63 mg). Anal. Calc. for $C_{106}H_{101}N_5Na_2Ni_6O_{25}$: C, 56.8; H, 4.5; N, 3.1. Observed: C, 56.4; H, 4.3; N, 3.1. IR mid/cm^{-1}: ν(O–H) 3411 (w), ν(N–H) 3179 (w), ν(C_{ar}–H) 3058, 3020 (w), ν(C–H) 2970, 2934, 2876 (w), ν(C=O) 1614 (*vs.*), ν(C=N), ν(C=C) 1597, 1537 (*vs.*), ν(C–O) 1223 (s).

General methods

Elemental analysis (C, H, N) was performed on a Thermo-Scientific Flash 2000 CHNS–O Analyser. The infrared spectrum of the complex was recorded on a ThermoNicolet NEXUS 670 FT-IR spectrometer using the ATR technique on a diamond plate in the range of 400–4000 cm^{-1}. The magnetic data were measured on powdered samples using a PPMS Dynacool system (Quantum Design) with VSM option. Experimental data were corrected for the diamagnetism of the constituent atoms by using Pascals' constants and for the diamagnetism of the sample holder.

X-ray diffraction analysis. X-ray diffraction experiment on the selected crystal of **1** was performed on an Xcalibur™2 diffractometer (Oxford Diffraction Ltd.) equipped with a Sapphire2 CCD detector using Mo-Kα radiation at 150 K. The CrysAlis program package (version 1.171.33.52, Oxford Diffraction) was used for data collection and reduction.[27] The molecular structure was solved by direct methods SHELXS-2014 and all non-hydrogen atoms were refined anisotropically on F^2 using full-matrix least-squares procedure SHELXL-2014.[28] The hydrogen atoms were found in differential Fourier maps (except for those mentioned below) and their parameters were refined using a riding model with U_{iso}(H) 1.2 (CH, CH_2, OH) or 1.5 (CH_3) U_{eq}(C). Non-routine aspects of the structure refinement are as follows: one propyl group of the Pr_3NH^+ cation is disordered over two positions. The positions of the hydrogen atoms belonging to the OH groups were not possible to determine from difference Fourier map reliably. Therefore, the hydrogen atoms were placed to the positions calculated by DFT method and their positions were restrained by SHELXL DFIX instructions between the particular hydrogen atom and hydrogen bonding acceptor atom (in both cases O22).

Theoretical methods. The DFT theoretical calculations were carried out with the ORCA 3.0.3 computational package.[39] Several DFT functionals, such as B3LYP,[29] PBE0,[30] TPSSh[31] and CAM-B3LYP[32] were used for calculations of the isotropic exchange constants J, following Ruiz's approach,[33] by comparing the energies of high-spin (HS) and broken-symmetry spin (BS) states. The polarized triple-ζ quality basis set def2-

TZVP(-f) proposed by Ahlrichs and co-workers was used for nickel, nitrogen and oxygen atoms and def2-SVP basis set for carbon and hydrogen atoms.[34] The calculations utilized the RI approximation with the decontracted auxiliary def2-TZV/J and def2-SVP Coulomb fitting basis set and the chain-of-spheres (RIJCOSX) approximation to exact exchange[35] as implemented in ORCA. Increased integration grids (Grid5 and Gridx5 in ORCA convention) and tight SCF convergence criteria were used in all calculations. The molecular fragment used in the calculations was extracted from the experimental X-ray structure and only hydrogen atoms positions were optimized with the PBE functional[36] together with atom-pairwise dispersion correction to DFT energy and the Becke–Johnson damping (D3BJ).[37] The calculated spin density was visualized with VESTA 3 program.[38]

Acknowledgements

We acknowledge the financial support from the National Programme of Sustainability I (LO1305) of the Ministry of Education, Youth and Sports of the Czech Republic, and from Palacký University in Olomouc (PrF_2016_007).

Notes and references

1 R. Sessoli, D. Gatteschi, A. Caneschi and M. A. Novak, *Nature*, 1993, **365**, 141–143.

2 (*a*) R. E. P. Winpenny, *Chem. Soc. Rev.*, 1998, **27**, 447–452; (*b*) Y. Wei, H. Hou, Y. Fan and Y. Zhu, *Eur. J. Inorg. Chem.*, 2004, **19**, 3946–3957; (*c*) R. Sessoli and A. K. Powell, *Coord. Chem. Rev.*, 2009, **253**, 2328–2341; (*d*) M. Nakano and H. Oshio, *Chem. Soc. Rev.*, 2011, **40**, 3239–3248; (*e*) L. Sorace, C. Benelli and D. Gatteschi, *Chem. Soc. Rev.*, 2011, **40**, 3092–3104; (*f*) D. N. Woodruff, R. E. P. Winpenny and R. A. Layfield, *Chem. Rev.*, 2013, **113**, 5110–5148; (*g*) A. K. Bar, C. Pichon and J.-P. Sutter, *Coord. Chem. Rev.*, 2016, **308**, 346–380.

3 (*a*) P.-H. Lin, N. C. Smythe, S. I. Gorelsky, S. Maguire, N. J. Henson, I. Korobkov, B. L. Scott, J. C. Gordon, R. T. Baker and M. Murugesu, *J. Am. Chem. Soc.*, 2011, **133**, 15806–15809; (*b*) S. Gomez-Coca, E. Cremades, N. Aliga-Alcalde and E. Ruiz, *J. Am. Chem. Soc.*, 2013, **135**, 7010–7018; (*c*) L. Chen, J. Wang, J.-M. Wei, W. Wernsdorfer, X.-T. Chen, Y.-Q. Zhang, Y. Song and Z.-L. Xue, *J. Am. Chem. Soc.*, 2014, **136**, 12213–12216; (*d*) S. Goméz-Coca, D. Aravena, R. Morales and E. Ruiz, *Coord. Chem. Rev.*, 2015, **289–290**, 379–392; (*e*) G. A. Craig and M. Murrie, *Chem. Soc. Rev.*, 2015, **44**, 2135–2147.

4 I. Nemec, R. Herchel, I. Svoboda, R. Boča and Z. Trávníček, *Dalton Trans.*, 2015, **44**, 9551–9960.

5 J. Miklovič, D. Valigura, R. Boča and J. Titiš, *Dalton Trans.*, 2015, **44**, 12484–12487.

6 (*a*) A. M. Ako, V. Mereacre, Y. Lan, W. Wernsdorfer, R. Clérac, C. A. Anson and A. K. Powell, *Inorg. Chem.*, 2010, **49**, 1–3; (*b*) T. Taguchi, W. Wernsdorgfer, K. A. Abboud and G. Christou, *Inorg. Chem.*, 2010, **49**, 10579–10589; (*c*) M. Ibrahim, Y. Lan, B. S. Bassil, Y. Xiang, A. Suchopar, A. K. Powell and U. Kortz, *Angew. Chem., Int. Ed.*, 2011, **50**, 4708–4711; (*d*) G. P. Guedes, S. Soriano, N. M. Comerlato, N. L. Spezialli, M. A. Novak and M. G. F. Vaz, *Inorg. Chem. Commun.*, 2013, **37**, 101–105; (*e*) A. E. Thuijs, P. King, K. A. Abboud and G. Christou, *Inorg. Chem.*, 2015, **54**, 9127–9137.

7 S. T. Ochsenbein, M. Murrie, E. Rusanov, H. Stoeckli-Evans, C. Sekine and H. U. Gude, *Inorg. Chem.*, 2002, **41**, 5133–5140.

8 J. Ribas-Arino, T. Baruah and M. R. Pederson, *J. Am. Chem. Soc.*, 2006, **128**, 9497–9505.

9 R. Herchel, I. Nemec, M. Machata and Z. Trávníček, *Dalton Trans.*, 2016, **45**, 18622–18634.

10 (*a*) G. Rogez, J.-N. Rebilly, A.-L. Barra, L. Sorace, G. Blondin, N. Kirchner, M. Duran, J. van Slageren, S. Parsons, L. Ricard, A. Marvilliers and T. Mallah, *Angew. Chem., Int. Ed.*, 2005, **44**, 1876–1879; (*b*) S. Gómez-Coca, E. Cremades, N. Aliaga-Alcalde and E. Ruiz, *Inorg. Chem.*, 2014, **53**, 676–678.

11 (*a*) C. Cadiou, M. Murrie, C. Paulsen, V. Villar, W. Wernsdorfer and R. E. P. Winpenny, *Chem. Commun.*, 2001, **24**, 2666–2667; (*b*) A. Bell, G. Aromí, S. T. Teat, W. Wernsdorfer and R. E. P. Winpenny, *Chem. Commun.*, 2005, **22**, 2808–2810; (*c*) G. Aromí, S. Parsons, W. Wernsdorfer, E. K. Brechin and J. L. McInnes, *Chem. Commun.*, 2005, **22**, 5038; (*d*) G. Aromí and E. K. Brechin, *Struct. Bonding*, 2006, **122**, 1–67; (*e*) R. T. W. Scott, L. F. Jones, I. S. Tidmarsh, *et al.*, *Chem.–Eur. J.*, 2009, **15**, 12389; (*f*) S. Petit, P. Neugebauer, G. Pilet, G. Chastanet, A.-L. Barra, A. B. Antunes, W. Wernsdorfer and D. Luneau, *Inorg. Chem.*, 2012, **51**, 6645–6654; (*g*) S. Hameury, L. Kayser, R. Pattacini, P. Rosa, A.-L. Barra and P. Braunstein, *ChemPlusChem*, 2015, **80**, 1312–1320.

12 (*a*) G. E. Lewis and C. S. Kraihanzel, *Inorg. Chem.*, 1983, **22**, 2895–2899; (*b*) A. J. Blake, C. M. Grant, S. Parsons, J. M. Rawson and R. E. P. Winpenny, *J. Chem. Soc., Chem. Commun.*, 1994, **20**, 2363–2364; (*c*) M. L. Tong, M. Monfort, J. M. Clemente-Juan, X.-M. Chen, X.-H. Bu, M. Ohba and S. Kitagawa, *Chem. Commun.*, 2005, **2**, 233–235; (*d*) D. Fouguet-Albiol, K. A. Abboud and G. Christou, *Chem. Commun.*, 2005, **34**, 4282–4284.

13 (*a*) V. Niel, V. A. Milway, L. N. Dawe, *et al.*, *Inorg. Chem.*, 2008, **47**, 176–189; (*b*) K. V. Shuvaev, S. S. Tandon, L. N. Dawe and L. K. Thompson, *Chem. Commun.*, 2010, **46**, 4755–4757; (*c*) L. K. Thompson and L. N. Dawe, *Coord. Chem. Rev.*, 2015, **289–290**, 13–31.

14 B. A. Breeze, M. Shanmugam, F. Tuna and R. E. P. Winpenny, *Chem. Commun.*, 2007, **48**, 5185–5187.

15 (*a*) M. Murrie, D. Biner, H. Stoeckli-Evans and H. U. Gudel, *Chem. Commun.*, 2003, **8**, 230–231; (*b*) J. Zhang, P. Teo, R. Pattacini, A. Kermagoret, R. Welter, G. Rogez, T. S. Andy Hor and P. Braustein, *Angew. Chem., Int. Ed.*, 2010, **49**, 4443–4446; (*c*) S. T. Meally, C. McDonnald, G. Karotsis, G. S. Papaefstathiou, E. K. Brechin, P. W. Dunne, P. McArdle, N. P. Power and L. F. Jones, *Dalton Trans.*, 2010, **39**, 4809–4816; (*d*) S.-H. Zhang, N. Li, C.-M. Ge, C. Feng and L.-F. Ma, *Dalton Trans.*, 2011, **40**, 3000–3007.

16 M. A. Halcrow, J.-S. Sun, J. C. Huffman and G. Christou, *Inorg. Chem.*, 1995, **34**, 4167–4177.

17 (*a*) E. Loukopoulos, B. Berkoff, K. Griffiths, V. Keeble, V. N. Dokorou, A. C. Tsipis, A. Escuer and G. E. Kostakis,

CrystEngComm, 2015, **17**, 6753–6764; (*b*) K. Griffiths, A. Escuer and G. E. Kostakis, *Struct. Chem.*, 2016, **27**, 1703–1714.

18 (*a*) I. Nemec, M. Machata, R. Herchel, R. Boča and Z. Trávníček, *Dalton Trans.*, 2012, **41**, 14603–14610; (*b*) P. Bag, J. Goura, V. Mereacre, G. Novitchi, A. K. Powell and V. Chandrasekhar, *Dalton Trans.*, 2014, **43**, 16366–16376; (*c*) K. Griffiths, V. N. Dokorou, J. Spencer, A. Abdul-Sada, A. Vargas and G. E. Kostakis, *CrystEngComm*, 2016, **18**, 704–713; (*d*) K. Griffiths, G. Novitchi and G. E. Kostakis, *Eur. J. Inorg. Chem.*, 2016, **2016**, 2750–2756; (*e*) H. Ke, W. Zhu, S. Zhang, G. Xie and S. Chen, *Polyhedron*, 2015, **87**, 109–116; (*f*) V. Chandrasekhar, P. Bag, W. Kroener, K. Gieb and P. Müller, *Inorg. Chem.*, 2013, **52**, 13078–13086; (*g*) W.-W. Kuang, C.-Y. Shao and P.-P. Yang, *J. Coord. Chem.*, 2015, **68**, 1412–1422; (*h*) E. Loukopoulos, B. Berkoff, A. Abdul-Sada, G. J. Tizzard, S. J. Coles, A. Escuer and G. E. Kostakis, *Eur. J. Inorg. Chem.*, 2015, **2015**, 2646–2649.

19 (*a*) R.-X. Zhang, Y.-X. Chang, H.-Y. Shen, W.-M. Wang, X.-P. Zhou, N.-N. Wang, J.-Z. Cui and H.-L. Gao, *Dalton Trans.*, 2016, **45**, 19117–19126; (*b*) W.-M. Wang, S.-Y. Wang, H.-X. Zhang, H.-Y. Shen, J.-Y. Zou, H.-L. Gao, J.-Z. Cui and B. Zhao, *Inorg. Chem. Front.*, 2016, **3**, 133–141; (*c*) H. Sun, L. Wu, W. Yuan, J. Zhao and Y. Liu, *Inorg. Chem. Commun.*, 2016, **70**, 164–167; (*d*) H. Zhang, J. Zhang, Y. Li, Y. Qin, Y. Chen, W. Liu, D. Gao and W. Li, *J. Coord. Chem.*, 2015, **68**, 2798–2809; (*e*) W.-W. Kuang, L.-L. Zhu, Y. Xu and P.-P. Yang, *Inorg. Chem. Commun.*, 2015, **61**, 169–172; (*f*) W.-M. Wang, S.-Y. Wang, H.-X. Zhang, B. Zhao, J.-Y. Zou, H.-L. Gao and J.-Z. Cui, *Inorg. Chim. Acta*, 2016, **439**, 106–110; (*g*) W.-M. Wang, H.-X. Zhang, S.-Y. Wang, H.-Y. Shen, H.-L. Gao, J.-Z. Cui and B. Zhao, *Inorg. Chem.*, 2015, **54**, 10610–10622; (*h*) K. C. Mondal, G. E. Kostakis, Y. Lan, W. Wernsdorfer, C. E. Anson and A. K. Powell, *Inorg. Chem.*, 2011, **50**, 11604–11611.

20 P. J. van Konigsbruggen, Y. Maeda and H. Oshio, *Top. Curr. Chem.*, 2004, **233**, 259–324.

21 (*a*) S. Saha, S. Pal, C. J. Gómez-García, J. M. Clemente-Juan, K. Harms and H. P. Nayek, *Polyhedron*, 2014, **74**, 1–5; (*b*) P. S. Perlepe, A. A. Athanasopoulou, K. I. Alexopoulou, C. P. Raptopoulou, V. Psycharis, A. Escuer, S. P. Perlepes and T. C. Stamatatos, *Dalton Trans.*, 2014, **43**, 16605–16609.

22 K. I. Alexopoulou, A. Terzis, C. P. Raptopoulou, V. Psycharis, A. Escuer and S. P. Perlepes, *Inorg. Chem.*, 2015, **54**, 5615–5617.

23 (*a*) R. Herchel, I. Nemec, M. Machata and Z. Trávníček, *Inorg. Chem.*, 2015, **54**, 8625–8638; (*b*) J.-D. Leng, S.-K. Xing, R. Herchel, J.-L. Liu and T. L. Ming, *Inorg. Chem.*, 2014, **53**, 5458–5466; (*c*) L. Mathivathanan, K. Al-Ameed, K. Lazarou, Z. Trávníček, Y. Sanakis, R. Herchel, J. E. McGrady and R. G. Raptis, *Dalton Trans.*, 2015, **44**, 20685–20691.

24 A. Das, F. J. Klinke, S. Demeshko, S. Meyer, S. Dechert and F. Meyer, *Inorg. Chem.*, 2012, **51**, 8141–8149.

25 R. Boča, *Coord. Chem. Rev.*, 2004, **248**, 757–815.

26 T. Tunc, M. Sari, M. Sadikoglu and O. Büyükgüngör, *J. Chem. Crystallogr.*, 2009, **39**, 672–676.

27 *CrysAlis CCD and CrysAlis RED, Version 1.171.33.52*, Oxford Diffraction Ltd, England, 2009.

28 G. M. Sheldrick, *Acta Crystallogr., Sect. A: Found. Adv.*, 2015, **71**, 3–8.

29 (*a*) A. D. Becke, *Phys. Rev. A: At., Mol., Opt. Phys.*, 1988, **38**, 3098–3100; (*b*) C. Lee, W. Yang and R. G. Parr, *Phys. Rev. B: Condens. Matter Mater. Phys.*, 1988, **37**, 785–789; (*c*) P. J. Stephens, F. J. Devlin, C. F. Chabalowski and M. J. Frisch, *J. Phys. Chem.*, 1994, **98**, 11623–11627.

30 C. Adamo and V. Barone, *J. Chem. Phys.*, 1999, **110**, 6158–6170.

31 V. N. Staroverov, G. E. Scuseria, J. Tao and J. P. Perdew, *J. Chem. Phys.*, 2003, **119**, 12129–12137.

32 T. Yanai, D. P. Tew and N. C. Handy, *Chem. Phys. Lett.*, 2004, **393**, 51–57.

33 (*a*) E. Ruiz, J. Cano, S. Alvarez and P. Alemany, *J. Comput. Chem.*, 1999, **20**, 1391–1400; (*b*) E. Ruiz, A. Rodríguez-Fortea, J. Cano, S. Alvarez and P. Alemany, *J. Comput. Chem.*, 2003, **24**, 982–989.

34 F. Weigend and R. Ahlrichs, *Phys. Chem. Chem. Phys.*, 2005, **7**, 3297–3305.

35 (*a*) F. Neese, F. Wennmohs, A. Hansen and U. Becker, *Chem. Phys.*, 2009, **356**, 98–109; (*b*) R. Izsak and F. Neese, *J. Chem. Phys.*, 2011, **135**, 144105.

36 J. P. Perdew, K. Burke and M. Ernzerhof, *Phys. Rev. Lett.*, 1996, **77**, 3865–3868.

37 S. Grimme, J. Antony, S. Ehrlich and H. Krieg, *J. Chem. Phys.*, 2010, **132**, 154104.

38 K. Momma and F. Izumi, *J. Appl. Crystallogr.*, 2011, **44**, 1272–127639.

39 F. Neese, *Wiley Interdiscip. Rev.: Comput. Mol. Sci.*, 2012, **2**, 73–78.